Chapter 4b

Alterations in miR34a-5p by CORM-A1 improves mitochondrial biogenesis and function in atherosclerosis

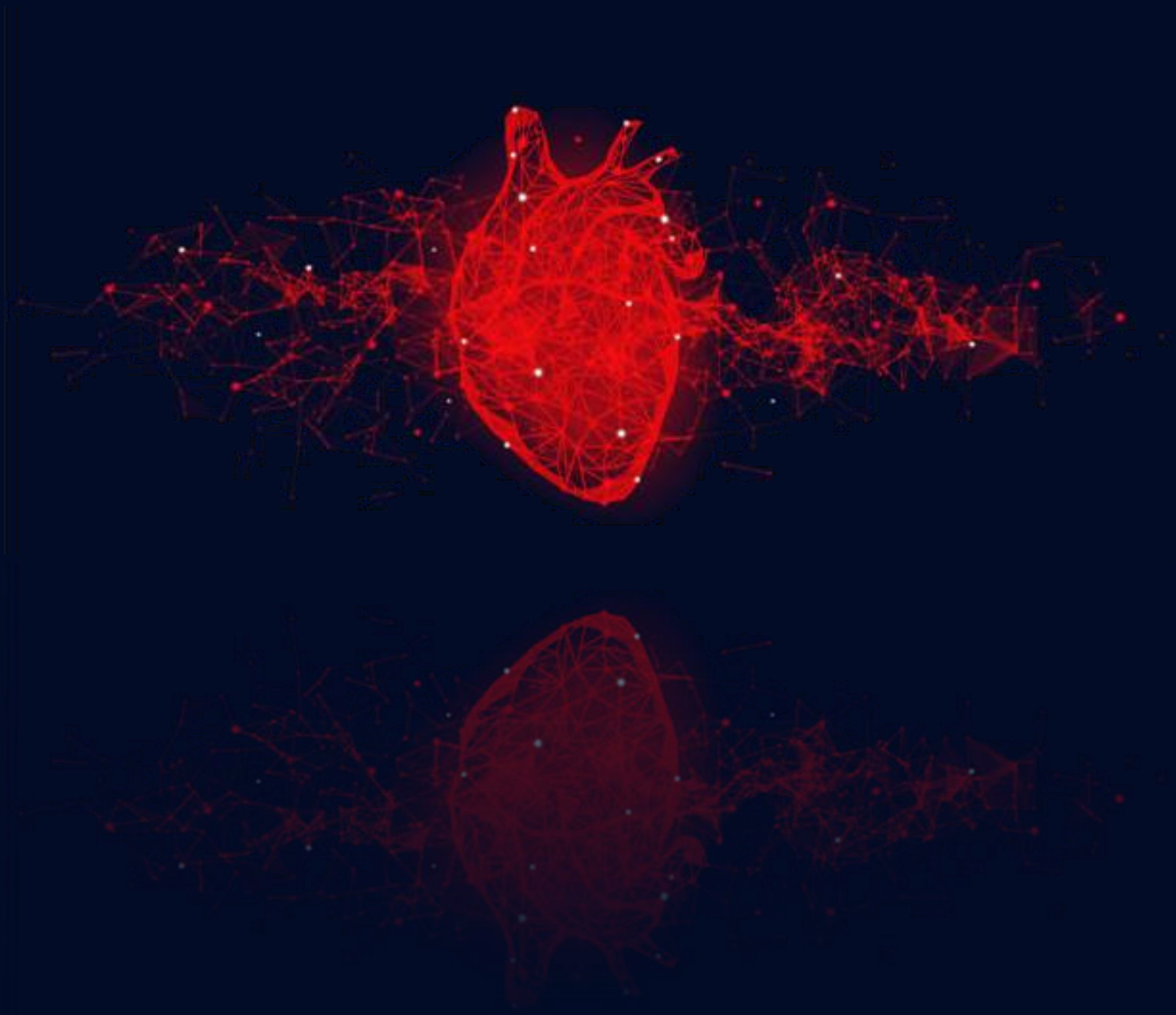

Introduction

Atherosclerosis is a complex multifactorial and progressive pathology with no clear demarcations of stages of initiation or progression. There have been several attempts to demarcate and mark the correct series of events in this progressive etiology as discussed in general introduction of the thesis. Presently, 2 different processes are believed to play a decisive role in the pathogenesis: inflammation and lipoprotein metabolism. Studies have identified prominent role of mitochondria in regulation of inflammatory processes, inflammasome assemblies and cellular metabolism (Gurung *et al.*, 2015). Normal mitochondrial function is critical for cell survival that is determined by a proportional balance between mitophagy (autophagic degradation of mitochondria) and mitochondrial biogenesis (production, fission and fusion). Mitochondrial status is known to be impaired in atherogenic etiology, at times progressing up to mitophagy which is major contributing factor for generation of cellular reactive oxygen species (ROS) (Forrester *et al.*, 2018). Overexpression of mitochondrial antioxidant gene SOD2 is studied to offer protection against cardiac IR injury (Awad *et al.*, 2018). Increased production of ROS in mitochondria, accumulation of mitochondrial DNA damage, and progressive respiratory chain dysfunction are strongly associated with progression of atherosclerosis (Madamanchi and Runge, 2007; Zorov *et al.*, 2014). mtDNA damage not only correlates with the extent of atherosclerotic lesions in apolipoprotein E (apoE) knockout mice but precedes atherogenesis in young apoE knockout mice (Mercer *et al.*, 2010). Studies have shown that lowered aerobic capacity is a strong predictor of mortality in subjects with/without cardiovascular disorders (Wisløff *et al.*, 2005). Expression of OXPHOS genes, essential for aerobic respiration are lowered in atherosclerosis (Markin *et al.*, 2021). Therefore, presently exhaustive

number of studies are focusing on targeting mitochondrial status for ameliorating cardiovascular disorders.

Pathogenic regulation of mitochondria has also been attributed to miRNAs in various conditions including heart failure and aging (miR181c) (Das *et al.*, 2014), hypertrophy and myocardial infraction (miR1) (Boštjančič *et al.*, 2010), Alzheimer's disease (miR743a) (Prasad, 2017), placental hypoxia (miR210) (Luo *et al.*, 2016), hypoxia and mitophagy in brain (miR137) (Li *et al.*, 2014a), cancer (miR34a) (Li *et al.*, 2021) etc. Moreover, key genes for vital mitochondrial functions including electron transport chain (ETC), OXPHOS, mitochondrial antioxidants have also been shown to be regulated by various miRNAs. Apart from miRNA-based regulation of mitochondrial operations, circadian rhythms also play a key role in influencing cellular mito-dymanics. Mitochondrial biogenesis genes, *SIRT1* is under strict circadian control in normal physiology, as deciphered in Chapter 2 that is also in agreement to the published reports in other model systems as well. Further, functionality of mitochondria is also under circadian control viz. there is a circadian control over biogenesis of NAD^+, regulating mitochondrial energy production (Peek *et al.*, 2013). Oxygen consumption rate (OCR) evaluated from the whole cells or isolated mitochondria from livers of Bmal1 knockout (KO) mice or liver specific Bmal1 KO and Per1 Per2 double KO mice had shown lowered OCR values (Levine *et al.*, 2020). Moreover, detailed investigations showed that mitochondria of Bmal1 KO mice were bigger and round and maintained the morphology throughout, whereas the control mice showed morphogenic alterations synchronous to the time-of-day. These cycles of fission and fusion and consequently the rhythms of energy production are regulated by dynamin-related protein 1 (DRP1), which is a key mediator of fission. Notably, activity of DRP1 is induced by phosphorylation, which occurs in a circadian manner to drive mitochondrial network

fragmentation (Schmitt *et al.*, 2018). In turn, suppression of mitochondrial fission eliminates circadian ATP production and feeds back to the core circadian oscillator to regulate circadian rhythmicity. But the overall number of mitochondria is constant and independent of clock genes.

Circadian associated endogenous gasotransmitter CO, as studied in chapter 2, is also reported to contribute to mitochondrial function. CO binding to COX (Cytochrome a, a3) is reported to have improved oxidation rate (Yoshikawa *et al.*, 2012). In past decade CO has been ventured in as one of the potential therapeutants in several pathologies. CORMs have gained great popularity pertaining to their controlled release of CO into the biological system. One of the studies from our lab showcases therapeutic properties of CORM-A1 in non-alcoholic steatohepatitis by improving mitochondrial function (Upadhyay *et al.*, 2020). CO is also reported to trigger mitochondrial biogenesis by activation NRF1 that binds to TFAM-3 to initiate the process.

This compile of study talks about anti-atherogenic potential of CORM-A1 using three experimental models (endothelial cells, macrophages, and SD rat). Overall, the mechanism of miR34a-5p lowering by CORM-A1 and subsequent regulation of miR34a-5p – SIRT-1 – mitochondrial axis had resulted in an improved mitochondrial function and biogenesis in atherogenic pathology. The study envisages the anti-atherogenic potential of CORM-A1, delimiting the expression of miR34a-5p and subsequently improving cellular mitochondrial and redox status.

Methodology

In-vivo Experimentations

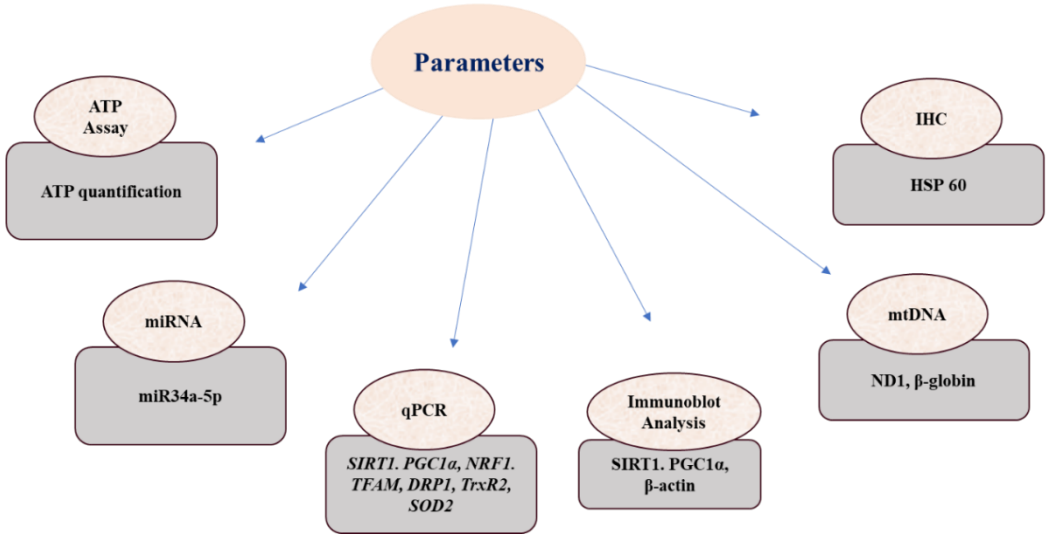

In-vitro Experimentations

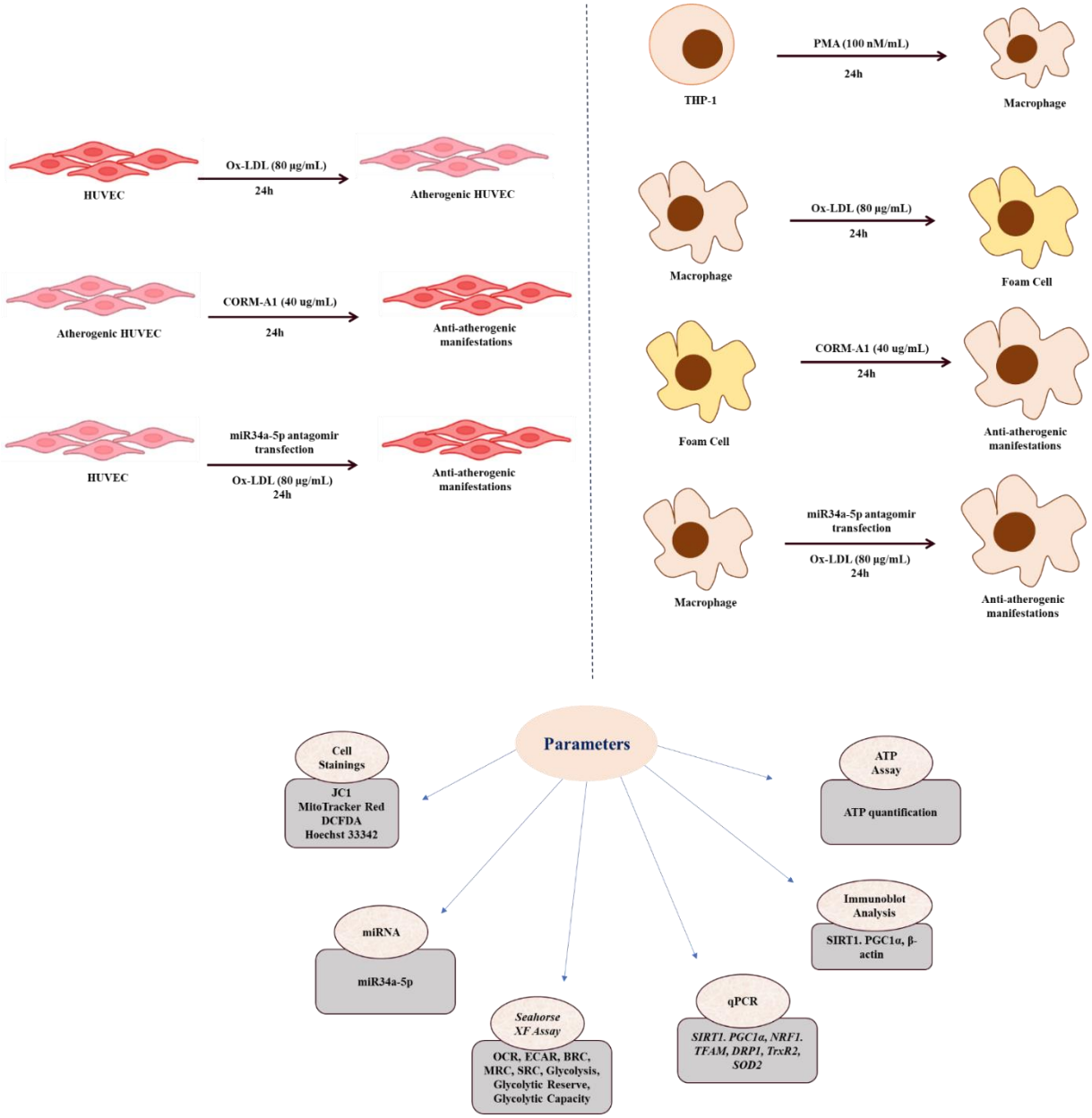

Results

Lowered miR34a-5p improves mitochondrial mass in atherogenic pathology.

Mitochondria has been studied to have vital impact on progression of atherosclerosis. Lowered mitochondrial number impairs cellular respiratory capacity as well as energy homeostasis and is directly related to cellular health. Herein, we assessed mitochondrial DNA (mtDNA) that is mitochondrial specific and indicates mitochondrial mass on thoracic aortae of SD rats from all the groups. mtDNA was evaluated by expression of mitochondrial encoded ND1 gene that was normalized with β-globin. The aortae of ath diet fed rats showed significantly lowered number of mtDNA as compared to that of the control. CORM-A1 treated rats exhibited improvement in terms of elevated number of mtDNA that were comparable to the control (Fig 4b.1a). Furthermore, we analysed mtDNA of ox-LDL and/or CORM-A1 treated HUVECs and MDMs by evaluating ND1 and normalizing it with 18s rRNA. Herein we observed results in agreement to the invivo data. Ox-LDL treated HUVECs and MDMs exhibited lowered mtDNA expression that was seen improved in CORM-A1 co-treated cells (Fig 4b.1b).

Further evaluation of mitochondria was done by MitoTracker Red staining in HUVECs and MDMs co-stained with Hoechst 33342 nuclear stain. Cells were observed and photographed under Nikon eclipse Ti2-E fluorescent microscope that clearly revealed decrement in mitochondrial mass in ox-LDL treated cells that was recovered comparable to control in CORM-A1 co-treated group in both HUVECs and MDMs (Fig 4b.2). Further validation was drawn from fluorescence quantification done using FiJi ImageJ software and represented graphically as CTCF values. Cumulatively, CORM-A1 improved mitochondrial mass in atherogenic conditions.

Elevated miR34a-5p in atherogenic milieu, lowers SIRT1 expression and consequent mitochondrial biogenesis, improvement on CORM-A1 treatment.

Cells co-treated with CORM-A1 harbouring lowered miR34a-5p showed elevated mitochondrial levels. Our in-silico investigating in agreement to published literature revealed that miR34a-5p has complementary site to the seed sequence in 3'UTR of *SIRT1* and can inhibit its expression. SIRT1 is vital in regulating mitochondrial biogenesis. To evaluate CORM-A1 mediated downregulation of miR34a-5p and consequential SIRT-1 elevation, we blocked miR34a-5p expression using cells transfected with miR34a-5p antagomiR. HUVEC and MDMs transfected with miR34a-5p antagomiR (IB HUVEC & IB MDMs) were treated with ox-LDL and compared to ox-LDL treated un-transfected cells. Atherogenic IB cells showed SIRT-1 titers comparable to that of the control, whereas atherogenic untransfected cells showed significantly lower levels of SIRT-1 presenting miR34a-5p as a causal link in lowering SIRT-1 levels (Fig 4b.3a). CORM-A1 co-treated cells, harboring lowered miR34a-5p accounted for elevated SIRT-1 titers as anticipated. PGC-1α is a nodal transcriptional regulator of mitochondrial that in turn is deacetylated and activated by SIRT1. Investigating its status in cells, a similar expression pattern was observed with PGC-1α, accounting for compromised mitochondrial biogenesis in cells harboring higher miR34a-5p titers at both the mRNA and protein levels (Fig 4b.3b-c). Thoracic aortae of SD rats also exhibited similar expression pattern of SIRT1 and PGC-1α in ath diet fed rats and CORM-A1 co-treated rats (Fig 4b.3d). Cumulatively, validating miR34a-5p mediated inactivation of 3'UTR of SIRT1 and consequently lowered expression along with PGC-1α, indicative of lowered mitochondrial biogenesis.

Elevated miR34a-5p in atherogenic milieu impends expression of mitochondrial biogenesis gene that are restored on CORM-A1 treatment.

Mitochondria is a vital dynamic organelle undergoing the process of fission and fusion pertaining to cellular energetics and health. There are multiple genes involved in this function. As mentioned above titers of SIRT-1 and PGC-1α were significantly depleted in pathogenic conditions in all the experimental models. Whereas *Nrf1* transcripts were elevated in invitro atherogenic systems but the same were found to be decreased in atherogenic aortae. CORM-A1 co-supplementation elevated expression of *Sirt-1, Pgc-1α* and *Nrf1* in all the disease models. We further checked for genes regulating mitochondrial fission (*Drp1*) and mitochondrial transcription (*Tfam*) that were significantly lowered in aortae of ath rats (Fig 4b.4c). Transcripts of *Tfam* were lowered in both the cells on ox-LDL treatment whereas Drp1 did not show any significant change in HUVEC. CORM-A1 treatment accounted for elevated *Drp1* and *Tfam* in all the experimental models (Fig 4b.4a, b). Collectively, the data shows that CORM-A1 mediated lowering of miR34a-5p, elevates SIRT-1 expression along with other mitochondrial biogenesis genes and enhances cellular mitochondrial mass.

Lowered miR34a-5p levels improves ox-LDL abrogated mitochondrial membrane potential and impends HSP60 expression

Redox imbalance in the vasculature culminates in elevation of redox sensitive miRNA-miR34a-5p and forms the basis of initiation of several detrimental pathophysiological processes including mitochondrial damage. Preliminary evidence on oxLDL mediated poor mitochondrial health was observed by JC-1 staining. Cells stained with JC-1 stain exhibits red and green florescence. Mitochondria with depolarized membrane having

lower mitochondrial membrane potential (MMP; Δψm) fluoresced in green color emitted by J-monomers, whereas mitochondria with healthy MMP fluoresced in red color emitted by J-aggregates. A prominent green florescence was observed in ox-LDL treated cells. whereas the CORM-A1 cotreated cells exhibited higher red/green florescence ratio depicting improved MMP in both the cell types. The florescence intensity was quantified as CTCF values that was in agreement to the cellular microscopic observations (Fig 4b.5).

Mitochondrial DAMPS are damage associated molecular patterns that are released from the mitochondria to the extracellular space triggering cell death. HSP60 is one such DAMP protein that is assessed herein for its expression. A damaged mitochondrial membrane provides gateway to HSP60, that typically functions inside the mitochondria. Excessive HSP60, when ooze out into the cytosol incurs harmful effect leading to endothelial dysfunction. Immunolocalization showed elevated HSP60 in atherogenic aortae that were reverted to normal on CORM-A1 treatment indicating restoration of healthy mitochondrial membrane (Fig 4b.6).

Lowered miR34a-5p levels improves ox-LDL abrogated mitochondrial and subsequent cellular redox status

Malfunction or inability of electron transport chain to operate at par with cellular energetic requirements results in formation of mtROS. Mitochondria is main source of generation of ROS. Several pathologies have reported mitochondrial ROS to be a detrimental insignia. Apart from number of mitochondria, mitochondrial status plays a vital role in dictating cellular health. Herein we assessed mitochondrial redox response capacity with mitochondrial specific antioxidant genes; *TrxR2* and *SOD2*. 3'UTR of

TrxR2 exhibits seed sequence complementary to miR34a-5p and have been reported to be regulated by the same suggesting miR-34a-5p mediated loss of antioxidants. Herein, oxLDL treated cells and aortae of ath diet fed SD rats, with elevated miR34a-5p levels, recorded lowered *TrxR2* and *SOD2* expression as anticipated. The same were found to be restored on CORM-A1 treatment, depicting improved mitochondrial redox status on lowering of redox sensitive miR34a-5p (Fig 4b.7a, b).

To establish whether the observed improvement in mitochondrial biogenesis and heath had increased cellular detoxification capacity we also assessed total cellular ROS status. HUVECs and MDMs treated with ox-LDL exhibited enhanced ROS, as evidenced by DCFDA staining. CORM-A1 treatment significantly lowered the same in both the cell types manifesting overall cellular improvement (Fig 4b.8a, b).

Depleting miR34a-5p titers in atherogenic pathology improves mitochondrial respiration and function

Mitochondrial function was assessed as total ATP production. ATP content estimated in thoracic aorta of ath diet fed SD and ox-LDL treated HUVEC and MDMs exhibited decrement in total cellular ATP. CORM-A1 treatment accounted for a significant increment in ATP levels (Fig 4b.9a, b).

miR34a-5p is also reported to decline mitochondrial function by binding to 3'UTR of cytochrome C and lowering its expression (Bukeirat *et al.*, 2016; Hu *et al.*, 2020). Disturbed cytochrome C expression impairs functioning of electron transport chain and compromises ATP production (Srinivasan and Avadhani, 2012). Mitochondrial respiration, oxidative stress and redox imbalance are symbolic in progression of proatherogenic changes and hence mitochondrial function was accessed by Seahorse

XF extracellular flux analyzer. Herein, the oxygen consumption rate (OCR) and glycolytic activity accessing lactic acid production and extracellular acidification rate (ECAR) were accessed in HUVEC and MDMs. oxLDL treatment accounted for significantly lowered OCR and ECAR values at all the time points (0-80 min). A significant improvement was observed in oxLDL + CORM-A1 treated group as evidenced by higher basal & maximal respiration capacity (BRC & MRC). Further, oligomycin mediated impact on ATP production and proton leak showed that oxLDL treatment caused a decrement in the said parameters. FCCP maximizes mitochondrial respiratory capacity and rotenone inhibits oxidative phosphorylation by blocking the complex 1. This step also enables us to detect the spare respiratory capacity. The same was found to be significantly lowered in oxLDL treated group and improved in oxLDL + CORM-A1 treated group. Addition of miR34a-5p antagomiRs to oxLDL treated group had resulted in significant improvement in OCR and ECAR values thus providing evidence on CORM-A1 orchestrating its action via miR34a-5p culminating in an improved mitochondrial respiration (Fig 4b.10 & Fig 4b.11).

(a)

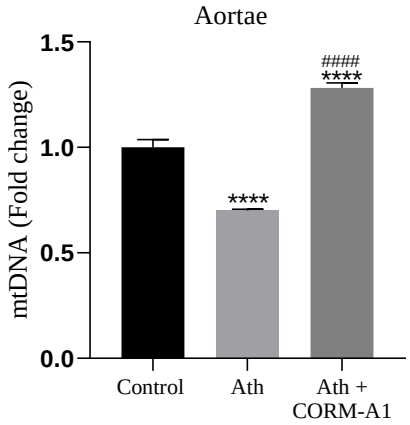

(b)

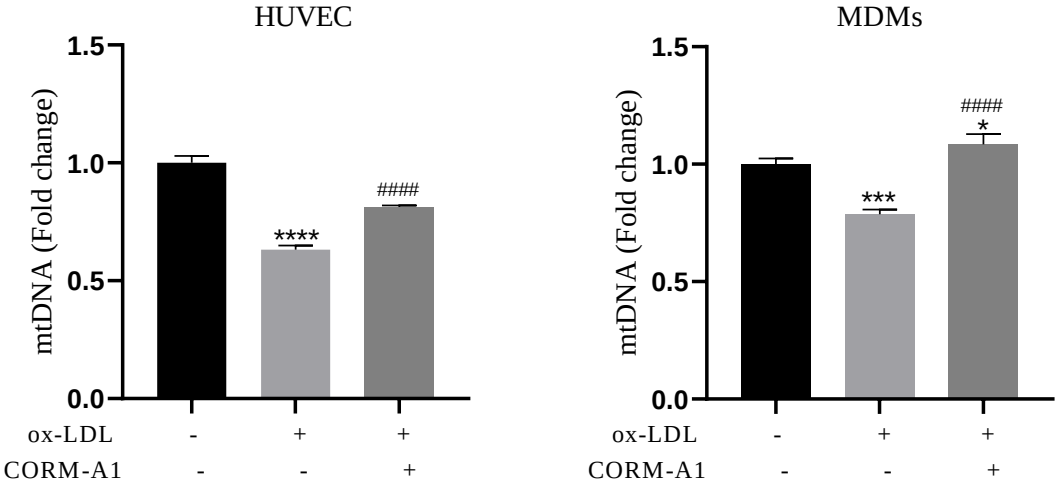

Fig. 4b.1: mitochondrial DNA was quantified with mitochondria specific ND1 gene normalized with nuclear encoded β-globin and 18sr RNA in (a) rat and (b) human (cells) respectively (n=2). Graphically represented as fold change. Results are expressed as mean ± S.E.M. *$p < 0.05$, **$p < 0.01$, ***$p < 0.001$ or ****$p < 0.0001$ is when compared to control group and $^{\#}p < 0.05$, $^{\#\#}p < 0.01$, $^{\#\#\#}p < 0.001$ or $^{\#\#\#\#}p < 0.0001$ when compared to atherogenic group.

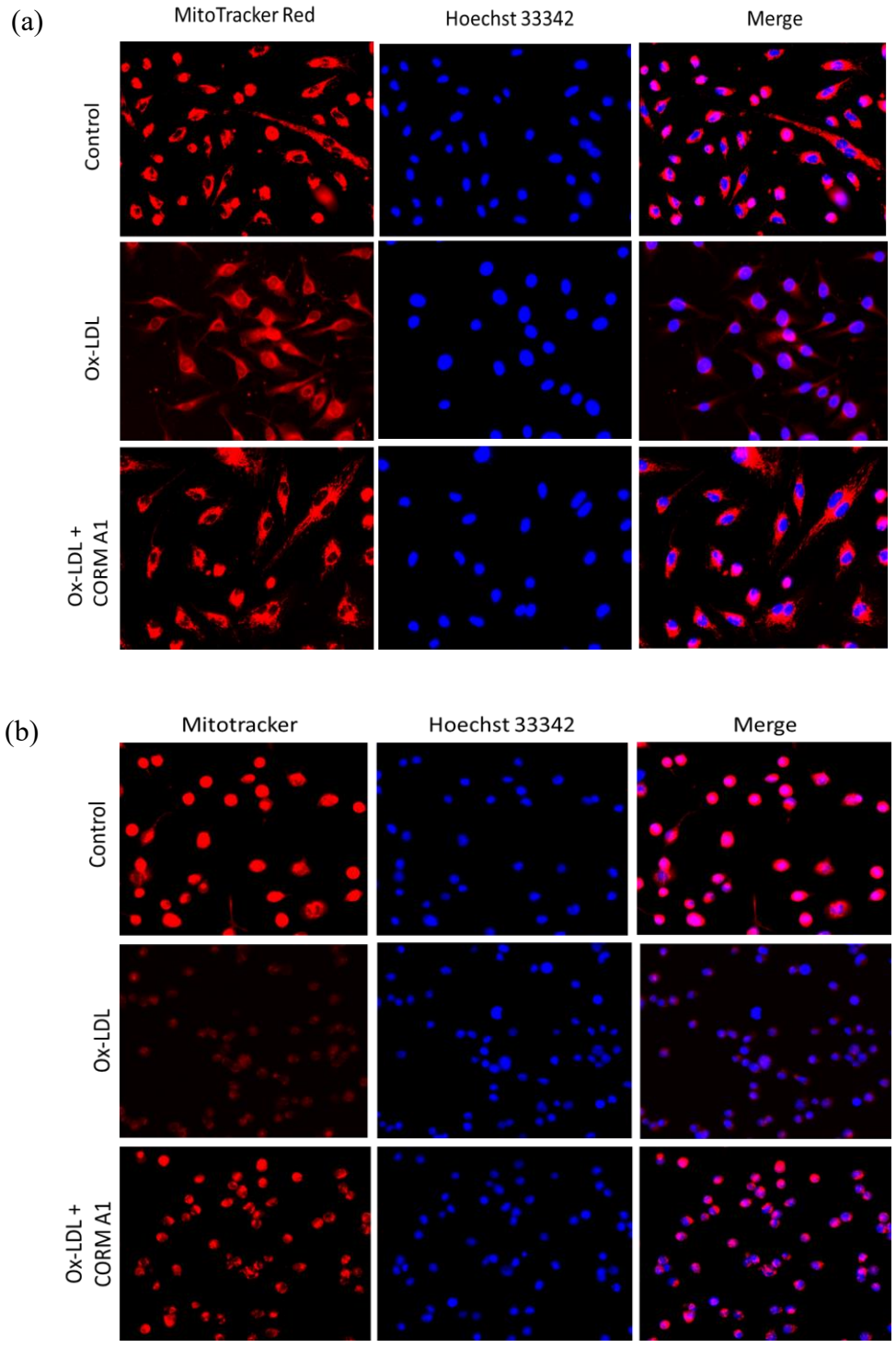

Fig. 4b.2: MitoTracker Red staining was done to assess mitochondrial mass in HUVEC (a) and MDMs (b). The cells were co-stained with Hoechst 33342 (nuclear stain) in blue. Imaging was done on FLoid Imaging station at 20X magnification. Higher red colored cells indicate more mitochondrial presence.

(a)

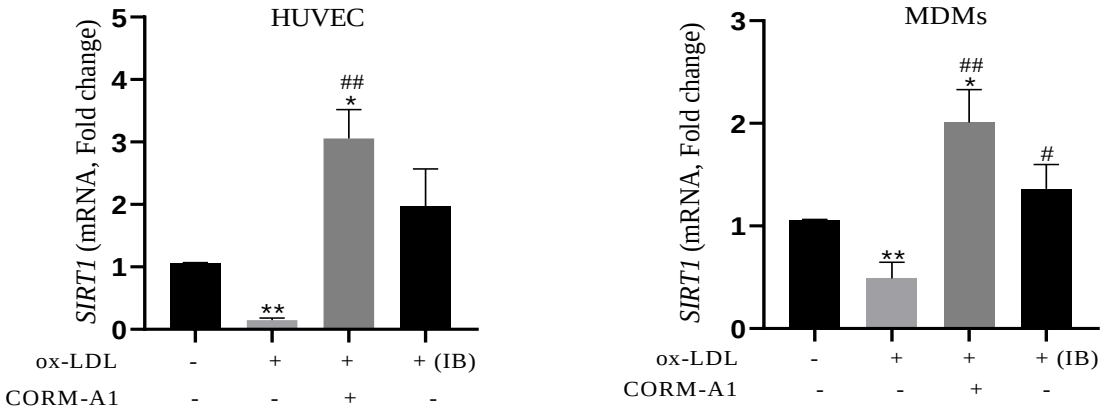
HUVEC
SIRT1 (mRNA, Fold change)
5
4
3
2
1
0
##
*
**
ox-LDL - + + + (IB)
CORM-A1 - - + -
MDMs
SIRT1 (mRNA, Fold change)
3
2
1
0
##
*
#
**
ox-LDL - + + + (IB)
CORM-A1 - - + -

(b)

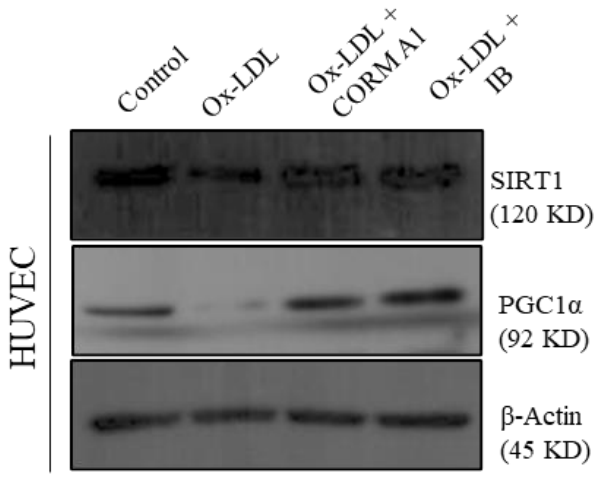
Control
Ox-LDL
Ox-LDL + CORM A1
Ox-LDL + IB
HUVEC
SIRT1 (120 KD)
PGC1α (92 KD)
β-Actin (45 KD)

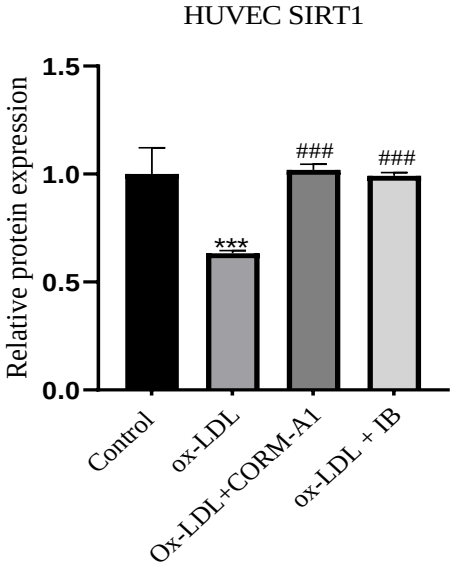
HUVEC SIRT1
Relative protein expression
1.5
1.0
0.5
0.0
***
###
###
Control
ox-LDL
Ox-LDL+CORM-A1
ox-LDL + IB

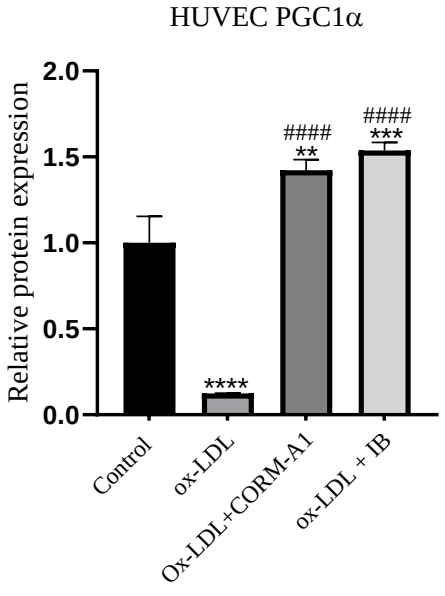
HUVEC PGC1α
Relative protein expression
2.0
1.5
1.0
0.5
0.0
****
####
**
####
***
Control
ox-LDL
Ox-LDL+CORM-A1
ox-LDL + IB

(c)

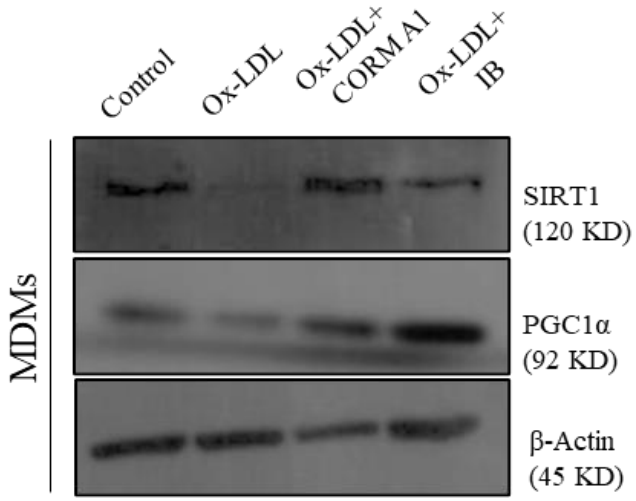
Control
Ox-LDL
Ox-LDL+ CORM A1
Ox-LDL+ IB
MDMs
SIRT1 (120 KD)
PGC1α (92 KD)
β-Actin (45 KD)

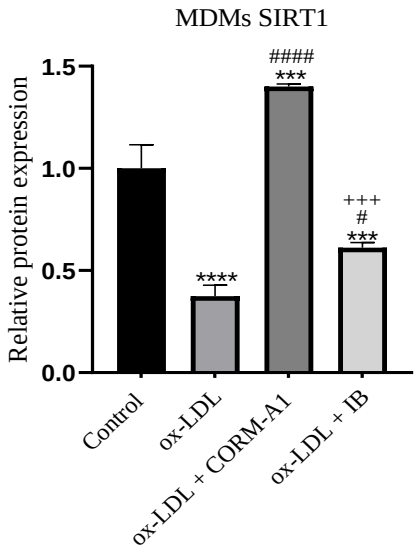
MDMs SIRT1
Relative protein expression
1.5
1.0
0.5
0.0
####
***
****
+++
#
***
Control
ox-LDL
ox-LDL + CORM-A1
ox-LDL + IB

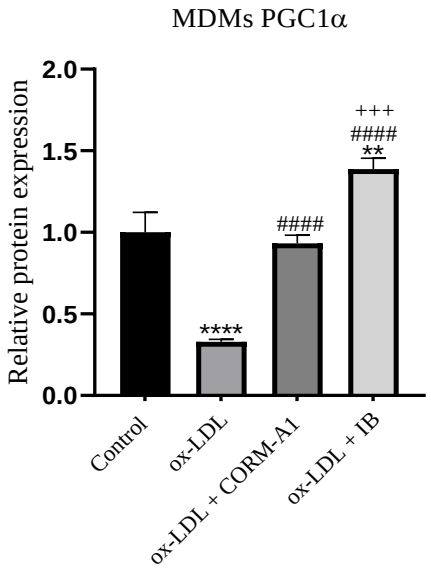
MDMs PGC1α
Relative protein expression
2.0
1.5
1.0
0.5
0.0
+++
####
**
####
****
Control
ox-LDL
ox-LDL + CORM-A1
ox-LDL + IB

(d)

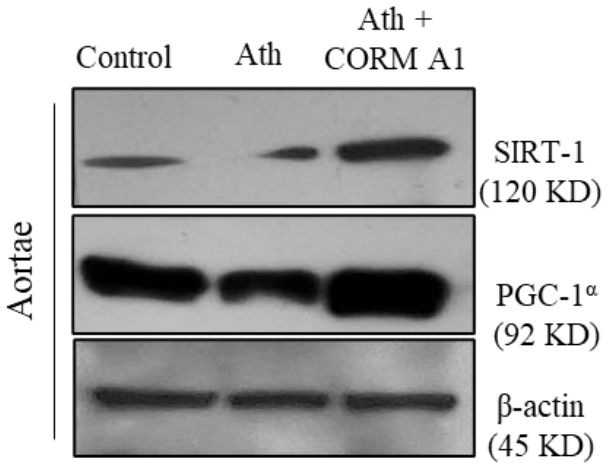
Control
Ath
Ath + CORM A1
Aortae
SIRT-1 (120 KD)
PGC-1α (92 KD)
β-actin (45 KD)

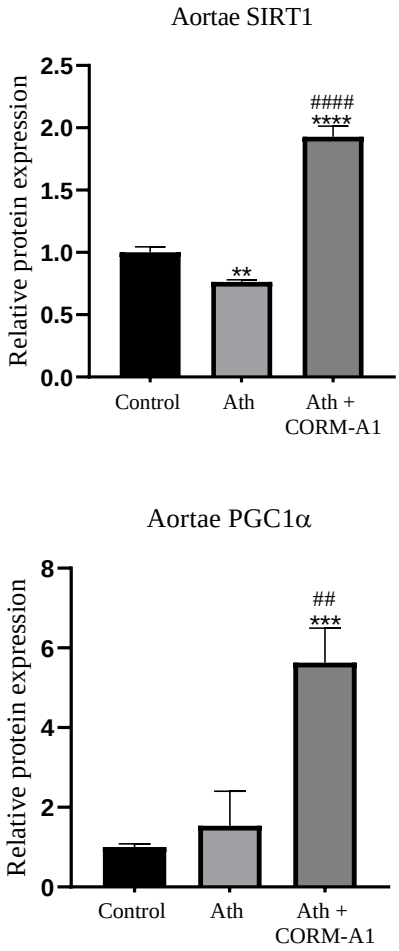

Fig. 4b.3: To evaluate miR34a-5p mediated response of CORM-A1 in atherogenic milieu, HUVECs and MDMs were transfected with miR34a-5p antagomiR in atherogenic model system. The (a) mRNA levels of *SIRT1* were quantified in HUVEC and MDMs respectively. Protein levels of SIRT1 and PGC1 α were assessed in (b) HUVEC (c) MDMs and (d) thoracic aortae of rats quantified (represented graphically). Proteins were normalized with housekeeping gene β-actin. Results are expressed as mean ± S.E.M. $*p < 0.05$, $**p < 0.01$, $***p < 0.001$ or ****p < 0.0001 is when compared to control group; $^{\#}p < 0.05$, $^{\#\#}p < 0.01$, $^{\#\#\#}p < 0.001$ or $^{\#\#\#\#}$p < 0.0001 when compared to atherogenic group and $^{+}p < 0.05$, $^{++}p < 0.01$, $^{+++}p < 0.001$ or $^{++++}$p < 0.0001 when compared to atherogenic group treated with CORM-A1.

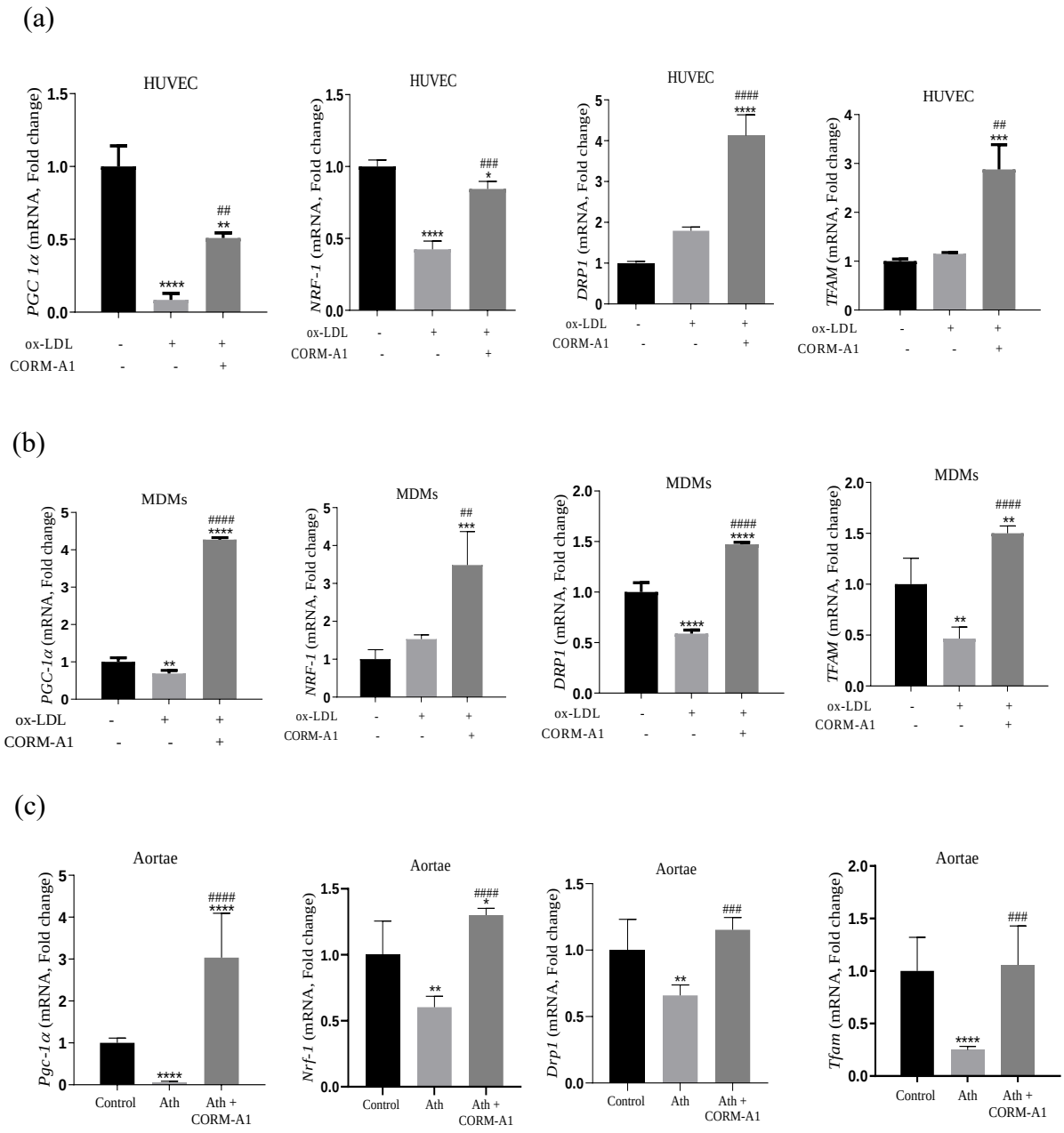

Fig. 4b.4: Transcriptional quantification of mitochondrial biogenesis genes was done by qPCR analysis in (a) HUVEC, (b) MDMs and (c) thoracic aorta (n=4). Results are expressed as mean ± S.E.M. *$p < 0.05$, **$p < 0.01$, ***$p < 0.001$ or ****$p < 0.0001$ is when compared to control group and $^{\#}p < 0.05$, $^{\#\#}p < 0.01$, $^{\#\#\#}p < 0.001$ or $^{\#\#\#\#}p < 0.0001$ when compared to atherogenic group.

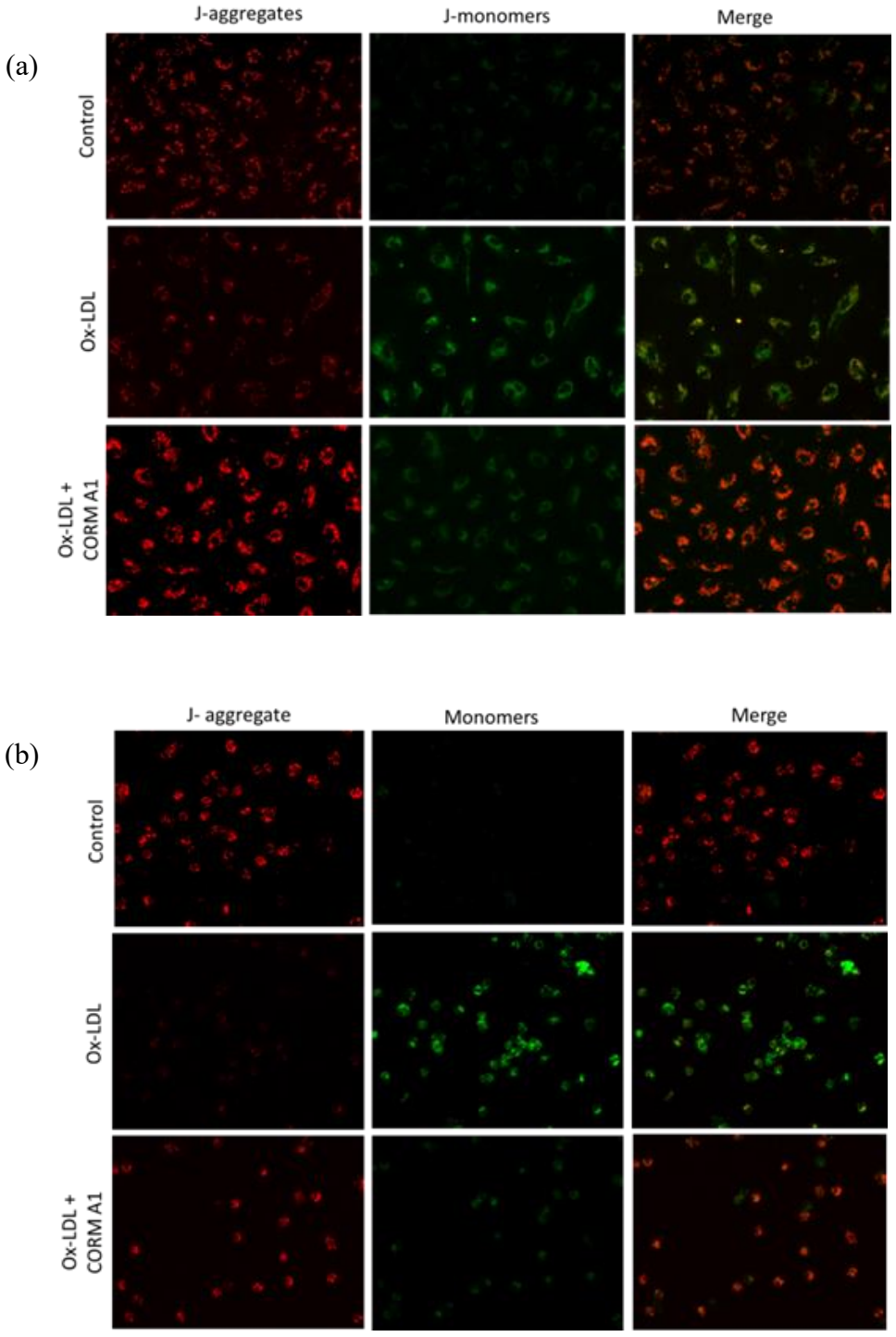

Fig. 4b.5: Mitochondrial membrane potential for HUVEC (a) and MDMs (b) was assessed with JC1 staining at the end of the experiment. Imaging was done under Floid Imaging station at 20x magnification. Red colored J-aggregates indicate healthy MMP whereas green colored J-monomers are indicative of impaired MMP.

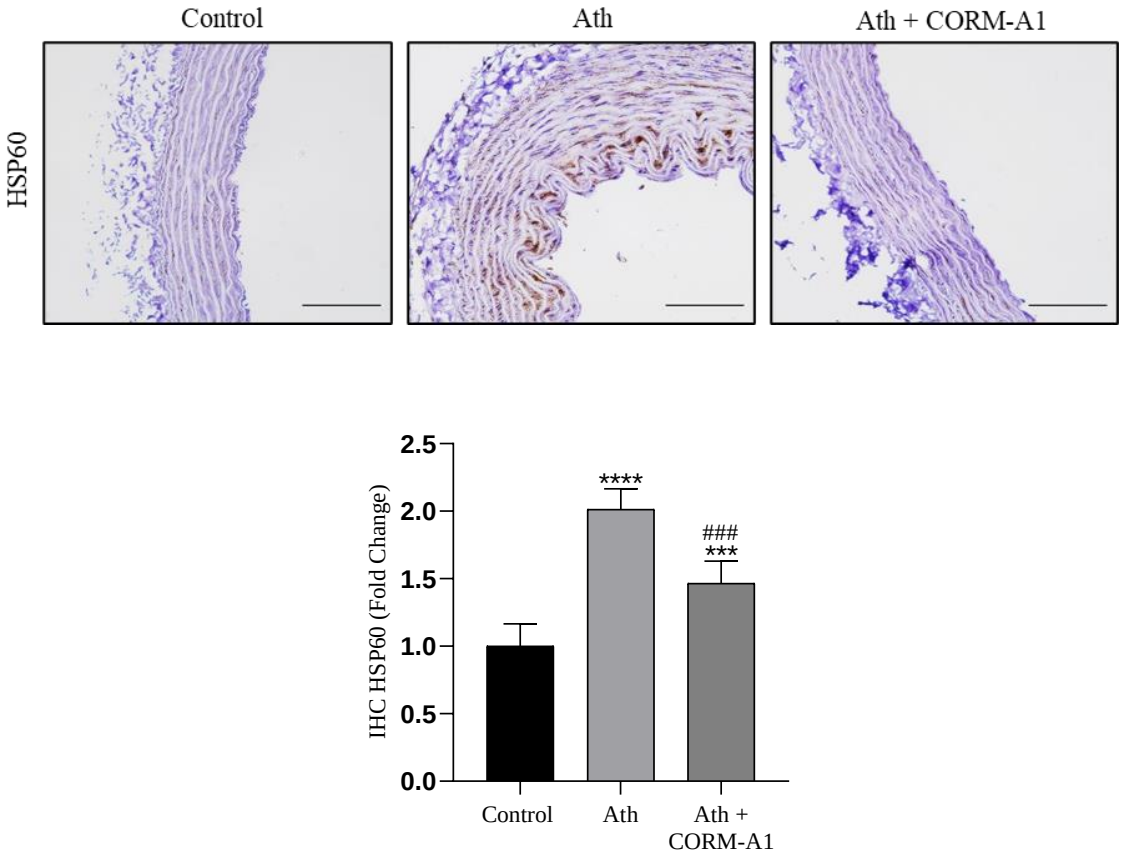

Fig. 4b.6: Thoracic aortae of SD were subjected for immunohistochemical analysis for HSP60 (n=3). Imagining was done under Nikon TiF2 Eclipse microscope at 20X magnification. Images were quantified using FiJi Image J software and represented graphically. Results are expressed as mean ± S.E.M. *$p < 0.05$, **$p < 0.01$, ***$p < 0.001$ or ****$p < 0.0001$ is when compared to control group and $^{\#}p < 0.05$, $^{\#\#}p < 0.01$, $^{\#\#\#}p < 0.001$ or $^{\#\#\#\#}p < 0.0001$ when compared to atherogenic group.

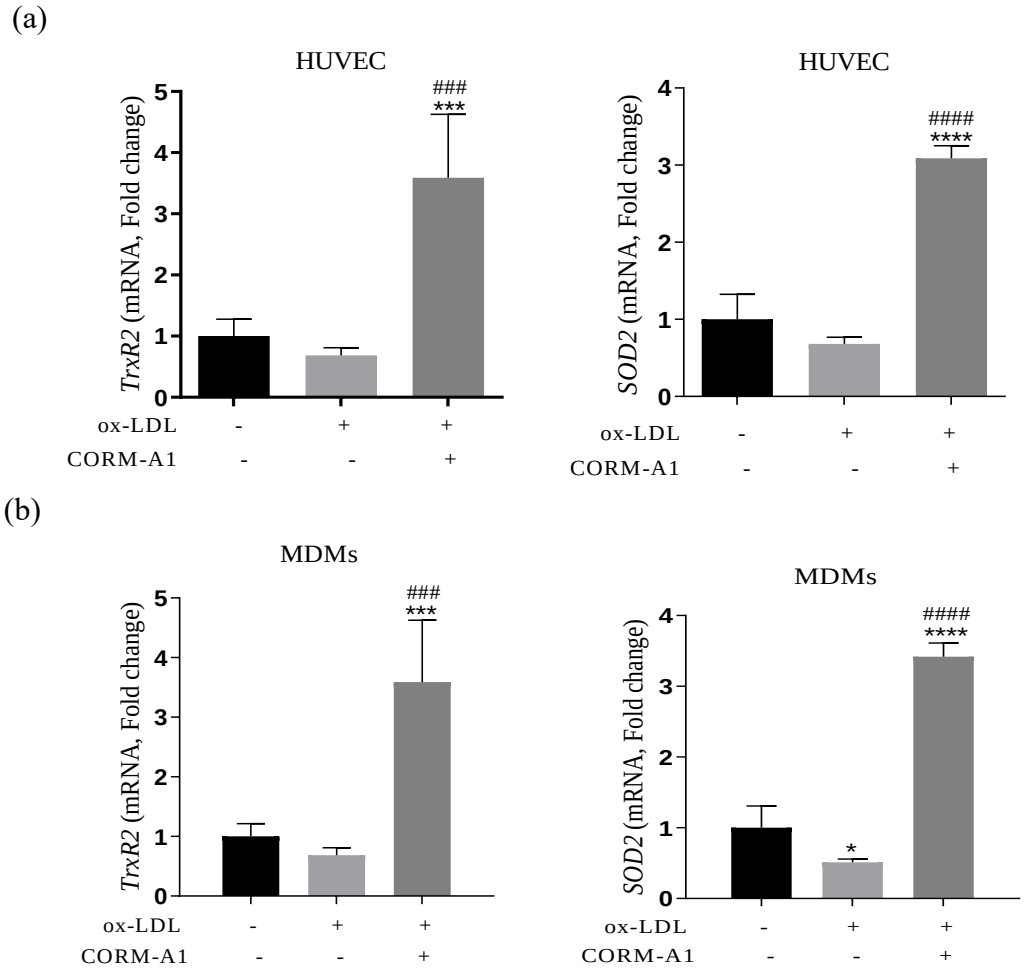

Fig. 4b.7: Mitochondrial antioxidant genes *TrxR2* and *SOD2* were analyzed at transcript levels by qPCR for (a) HUVEC and (b) MDMs (n=3). Results are expressed as mean ± S.E.M. *$p < 0.05$, **$p < 0.01$, ***$p < 0.001$ or ****$p < 0.0001$ is when compared to control group and $^{\#}p < 0.05$, $^{\#\#}p < 0.01$, $^{\#\#\#}p < 0.001$ or $^{\#\#\#\#}p < 0.0001$ when compared to atherogenic group.

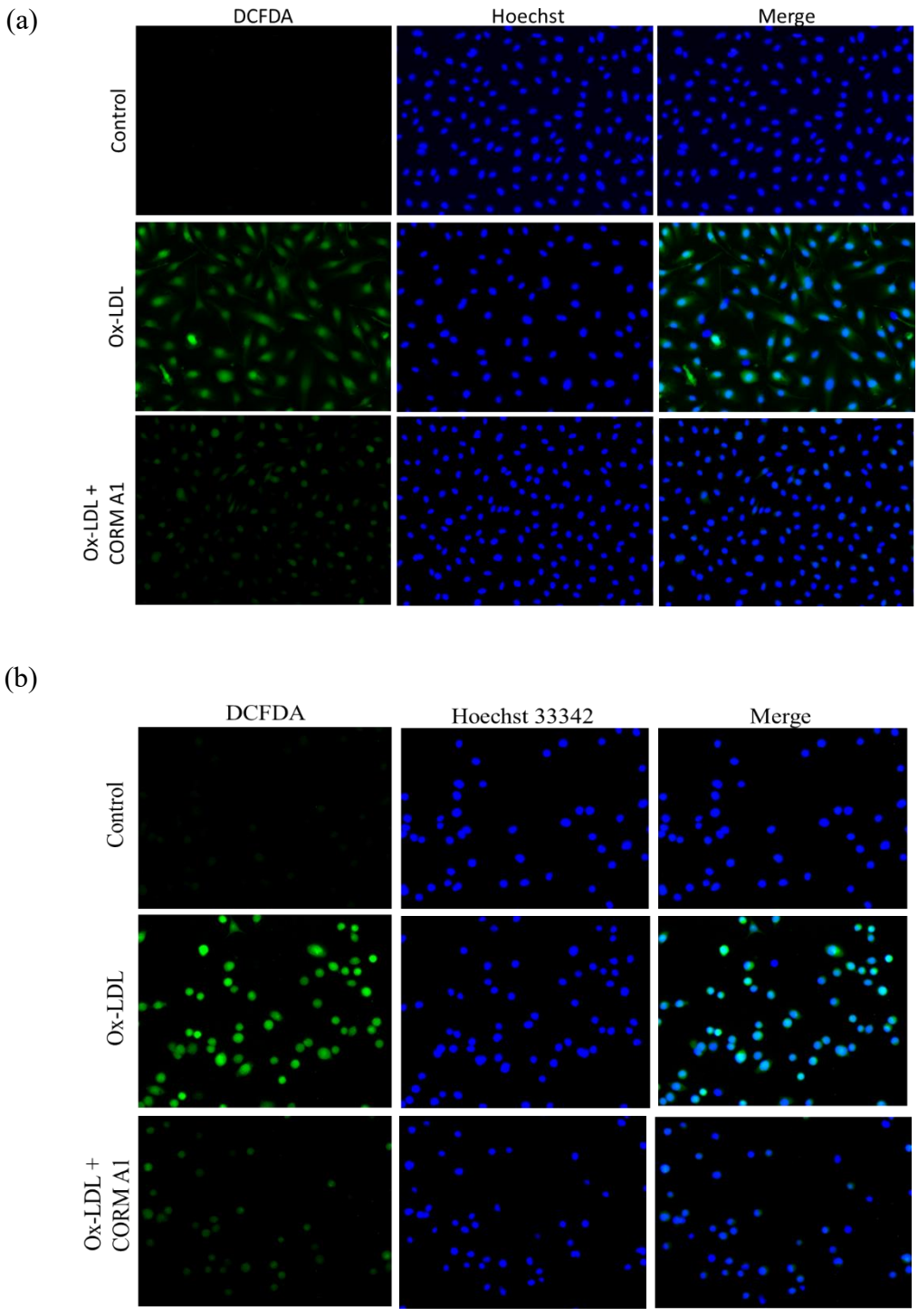

Fig. 4b.8: Cellular redox status was assessed by DCFDA staining, co-stained with Hoechst 33342 (nuclear Stain) to (a) HUVEC and (b) MDMs. Imaging was done using Floid Imaging station with 20X magnification. Higher green fluorescence intensity is indicative of elevated presence of cellular ROS.

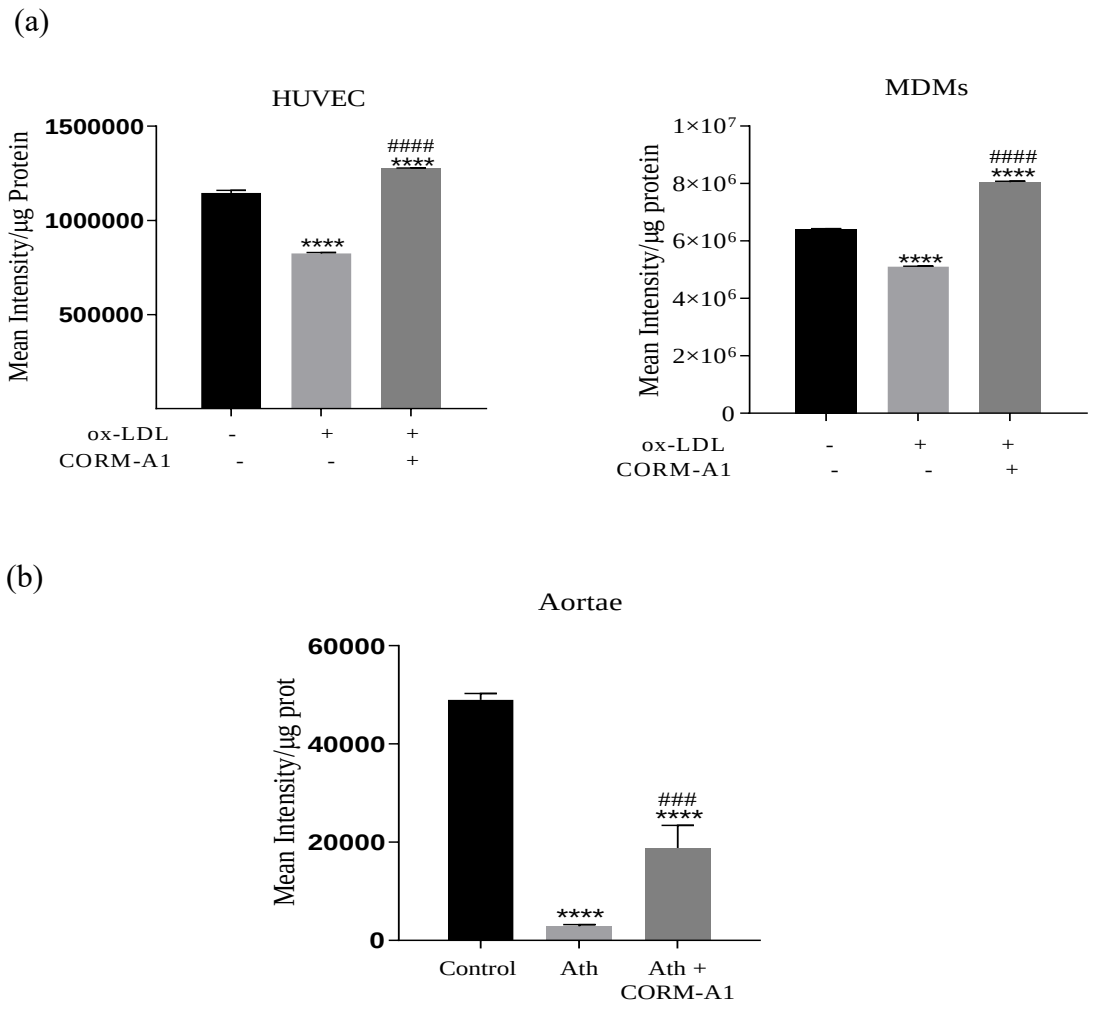

Fig. 4b.9: Mitochondrial functional analysis was by ATP quantification in (a) HUVEC and MDMs and (b) thoracic aortae of SD rats (n=3). Results are expressed as mean ± S.E.M. *$p < 0.05$, **$p < 0.01$, ***$p < 0.001$ or ****$p < 0.0001$ is when compared to control group and $^{\#}p < 0.05$, $^{\#\#}p < 0.01$, $^{\#\#\#}p < 0.001$ or $^{\#\#\#\#}p < 0.0001$ when compared to atherogenic group.

(a)

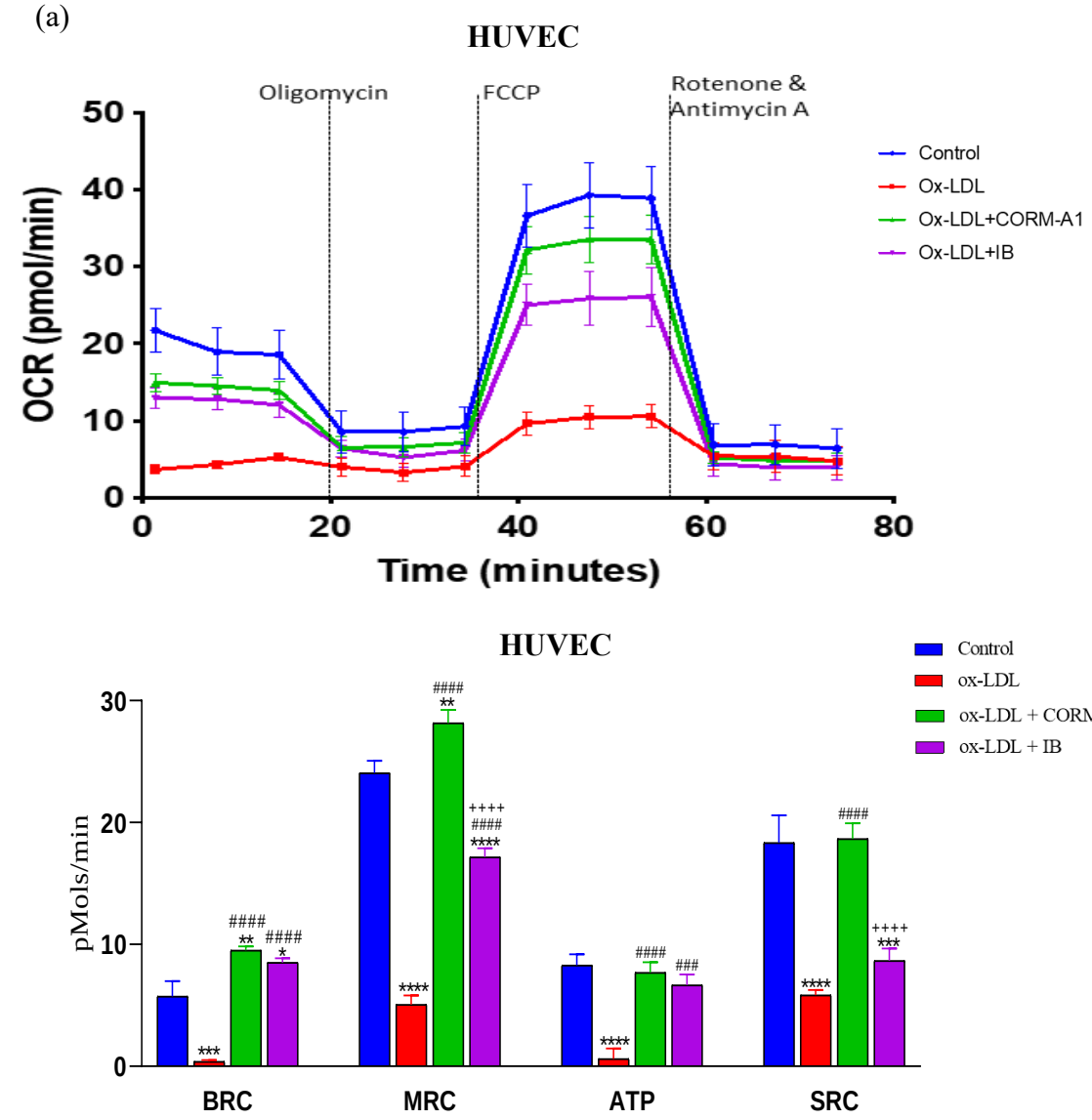
HUVEC
Oligomycin
FCCP
Rotenone &
Antimycin A
OCR (pmol/min)
Time (minutes)
Control
Ox-LDL
Ox-LDL+CORM-A1
Ox-LDL+IB
HUVEC
pMols/min
BRC
MRC
ATP
SRC
Control
ox-LDL
ox-LDL + CORM-A1
ox-LDL + IB

(b)

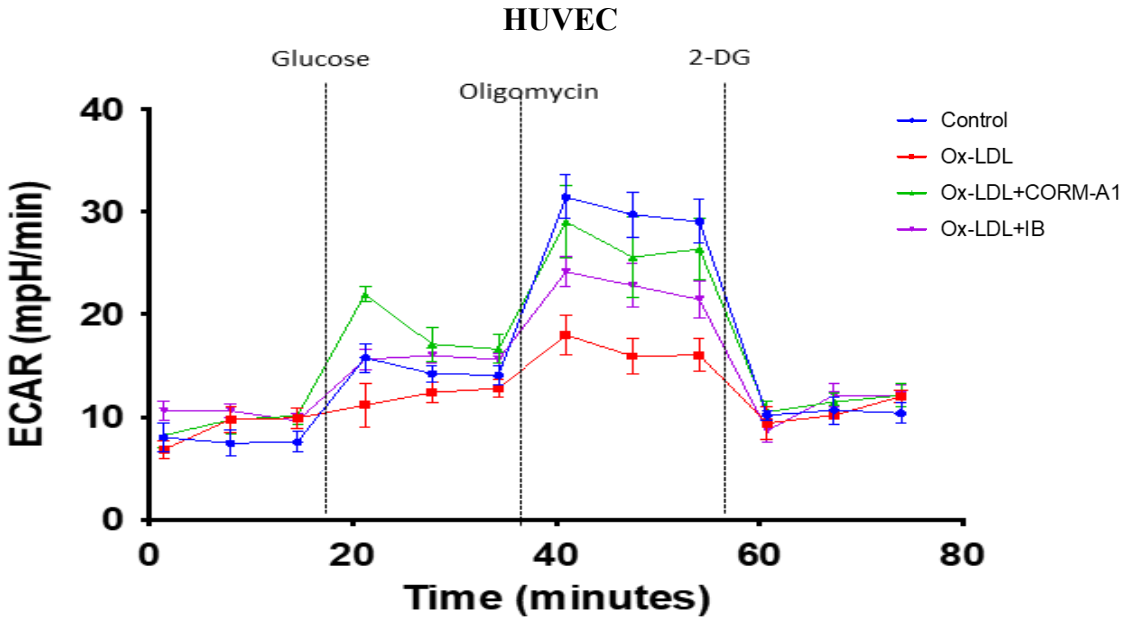
HUVEC
Glucose
Oligomycin
2-DG
ECAR (mpH/min)
Time (minutes)
Control
Ox-LDL
Ox-LDL+CORM-A1
Ox-LDL+IB

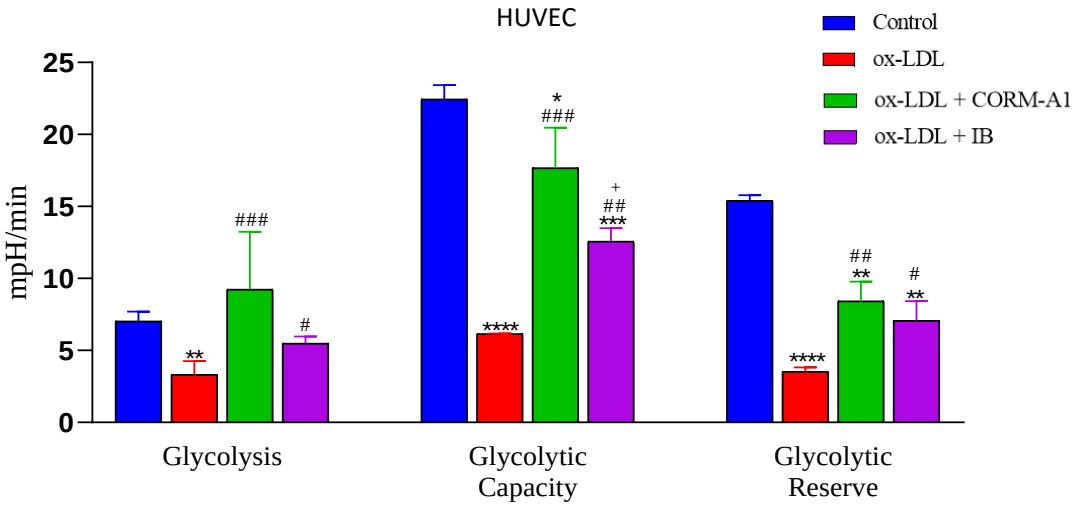

Fig. 4b.10: Seahorse XF Analyzer was used to assess mitochondrial status by quantifying (a) oxygen consumption rate (OCR) and further calculating Basal Respiratory Capacity (BRC), Maximal Respiratory Capacity (MRC), ATP and Spare Respiratory Capacity (SRC) and (b) extracellular acidification rate (ECAR) giving insight into glycolysis, glycolytic capacity, and glycolytic reserve of the HUVEC cells in real time. Results are expressed as mean ± S.E.M. *$p < 0.05$, **$p < 0.01$, ***$p < 0.001$ or ****$p < 0.0001$ is when compared to control group; $^{\#}p < 0.05$, $^{\#\#}p < 0.01$, $^{\#\#\#}p < 0.001$ or $^{\#\#\#\#}p < 0.0001$ when compared to atherogenic group and $^{+}p < 0.05$, $^{++}p < 0.01$, $^{+++}p < 0.001$ or $^{++++}p < 0.0001$ when compared to atherogenic group treated with CORM-A1.

(a)

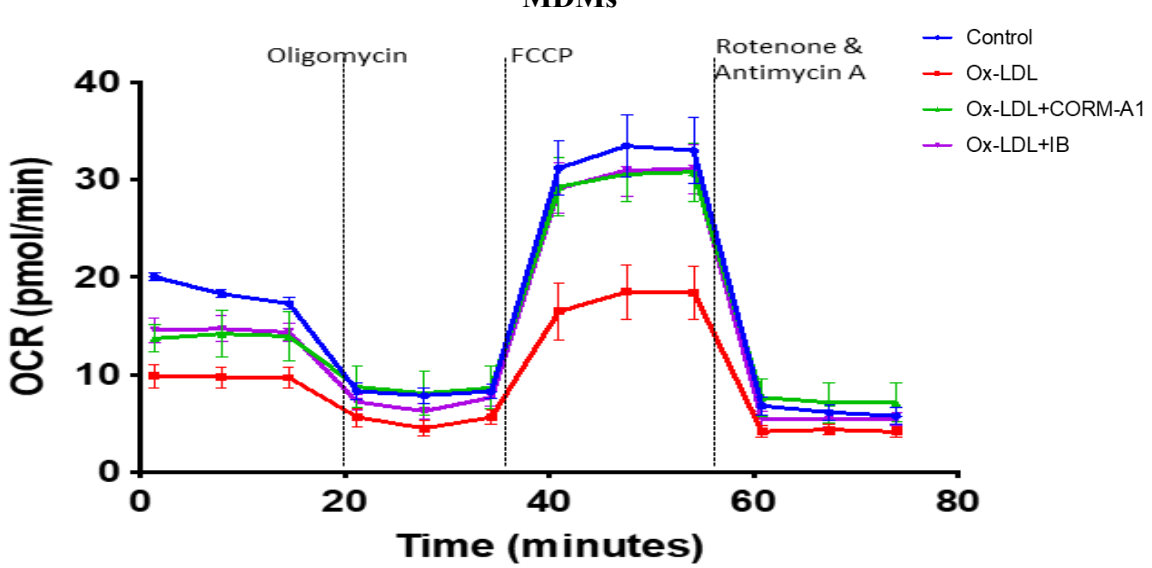
MDMs
Oligomycin
FCCP
Rotenone &
Antimycin A
Control
Ox-LDL
Ox-LDL+CORM-A1
Ox-LDL+IB
OCR (pmol/min)
0
10
20
30
40
0
20
40
60
80
Time (minutes)

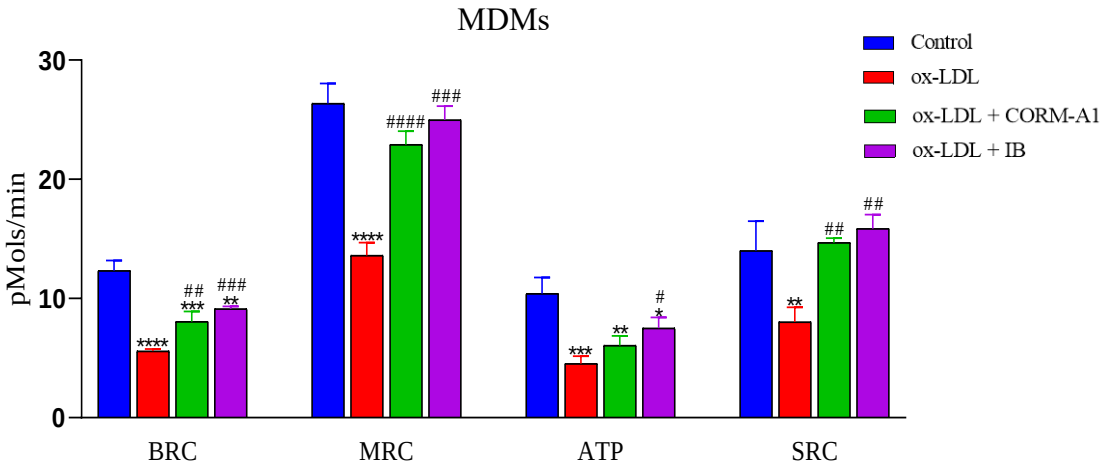
MDMs
Control
ox-LDL
ox-LDL + CORM-A1
ox-LDL + IB
pMols/min
0
10
20
30
BRC
MRC
ATP
SRC

(b)

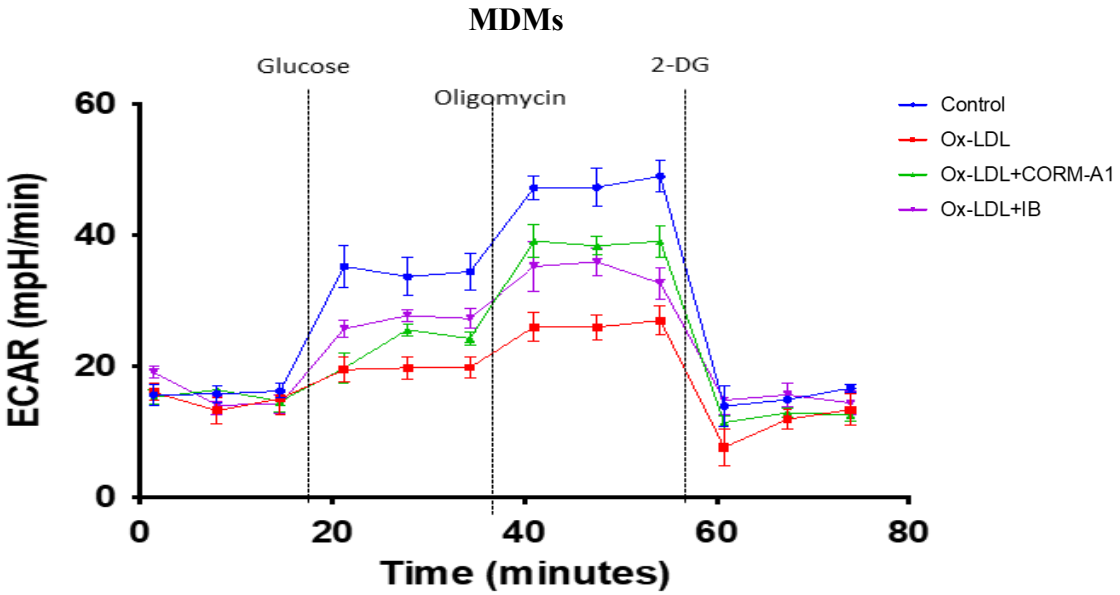
MDMs
Glucose
Oligomycin
2-DG
Control
Ox-LDL
Ox-LDL+CORM-A1
Ox-LDL+IB
ECAR (mpH/min)
0
20
40
60
0
20
40
60
80
Time (minutes)

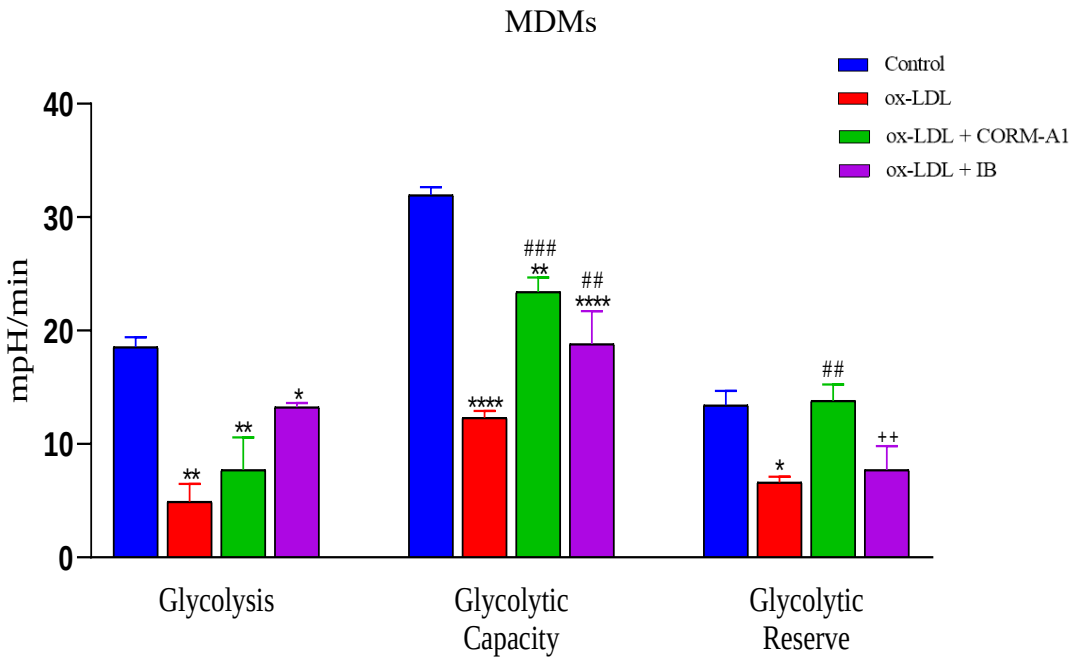

Fig. 4b.11: Seahorse XF Analyzer was used to assess mitochondrial status by quantifying (a) oxygen consumption rate (OCR) and further calculating Basal Respiratory Capacity (BRC), Maximal Respiratory Capacity (MRC), ATP and Spare Respiratory Capacity (SRC) and (b) extracellular acidification rate (ECAR) giving insight into glycolysis, glycolytic capacity, and glycolytic reserve of the MDM cells in real time. Results are expressed as mean ± S.E.M. $*p < 0.05$, $**p < 0.01$, $***p < 0.001$ or ****p < 0.0001 is when compared to control group; $^{\#}p < 0.05$, $^{\#\#}p < 0.01$, $^{\#\#\#}p < 0.001$ or $^{\#\#\#\#}$p < 0.0001 when compared to atherogenic group and $^{+}p < 0.05$, $^{++}p < 0.01$, $^{+++}p < 0.001$ or $^{++++}$p < 0.0001 when compared to atherogenic group treated with CORM-A1.

Discussion

miR34a-5p has been documented as oxidative stress response miRNA, regulating the expression of SIRT-1 that largely maintains cellular homeostasis. SIRT1 has been implicated as a molecular switch regulating endothelial health and disease by differentially controlling the expression of factors that confer anti-oxidative, anti-inflammatory, antithrombotic, vasodilatory and anti-proliferative effects in atherogenic ECs (Ministrini *et al.*, 2021). Herein we show CORM-A1 regulates miR34a-5p – SIRT-1 axis, facilitating a cellular redox shift and improvement, in atherogenic conditions. CORM-A1 treatment results in recovery of 3'UTR activity of SIRT-1 that facilitates mitochondrial biogenesis as evidenced by MitoTraker Red and mtDNA copy number. CO is reported to improve mitochondrial health and function in neuronal cells, hepatocytes, endothelial cells, and cardiomyocytes of isolated heart. Herein, oxLDL accumulation incurs ROS production, mitochondrial hyperpolarization and disrupted MMP that was effectively restored on CORM-A1 treatment, as evidenced by DCFDA and JC-1 staining in HUVECs and MDMs. Cells harbouring damaged mitochondria are exposed to the risk of, mitochondrial homed HSP60, leaking out into the cytosol. Excessive HSP60 leak into the cytosol is proatherogenic trait that promotes endothelial dysfunction and cell death (Na *et al.*, 2009). IHC staining showed CORM-A1 mediated lowering of HSP60 in luminal and sub-luminal region of atherogenic aortae promoting anti-atherogenic manifestations.

Mitochondrial redox status, regulated by TrxR2 and SOD2, is vital in regulating its health. Thonaujam *et al* showed that miR34a-5p binds to 3'UTR of TrxR2 and halts the protein expression, depressing mitochondrial status (Thounaojam *et al.*, 2019). Herein, ox-LDL/ ath diet group with elevated miR34a-5p showed lowered expression of TrxR2

and SOD2 that was restored on CORM-A1 treatment. Increased mitochondrial number and health imply towards efficient mitochondrial function that was accessed by ATP and seahorse assay. Higher ox-LDL accumulation in atherogenic cells, promote mitochondrial hyperpolarization and OXPHOS dysfunction leading to elevated cellular ROS. Ox-LDL treatment augmented depression in BRC & MRC coupled with lowered ATP production in atherogenic HUVECs and MDMs. CO is reported to orchestrate mitochondrial uncoupling via elevated proton leak, shifting cellular energy production from glycolysis back to OXPHOS. CORM-A1 treatment mitigated BRC and MRC in atherogenic HUVEC and MDMs further culminating in elevated ATP production. Mechanistic counteractive impact of CORM-A1 was further assessed in IB cells wherein MDMs showed maximal CORM-A1 operation via miR34a-5p. Whereas HUVECs exhibit corrective variance in IB and non-IB cells, implying towards a plausible mechanism wherein CORM-A1 mitigates via an alternative pathway along with miR34a-5p. Further, the data shows that CORM-A1 boosts overall cellular respiration in HUVECs whereas, a shift is observed in cellular energetics dependency from non-mitochondrial to mitochondrial respiration in case of MDMs. However, it is evident from the data that CORM-A1 mitigates mitochondrial respiration majorly via miR34a-5p in atherogenic HUVEC and MDMs.

These results suggest that miR34a-5p antagomir can be a viable therapeutic option for treating atherosclerosis. Moreover, the study also reveals that CORM-A1 can manifest its own multipronged effect by lowering miR34a-5p levels and improving mitochondrial respiration consequently improving cellular redox status in miR34a-5p – SIRT-1 – mitochondria dependent and independent manner. Proposing CORM-A1 as competent pharmacological option for atherosclerosis.